

Contents list available at CBIORE journal website

BIRE Journal of Emerging Science and Engineering

Journal homepage: https://journal.cbiore.id/index.php/jese/index



Investigations on co-gasification and combustion characteristics of coal biomass blend as an alternative transport fuel for tri-cycles

Benson Kariuki1*, Paul Njogu1; Joseph Kamau1, Robert Kinyua2, Reiner Malessa3, Sameer Bachani4

Abstract. Kenya discovered huge deposit of lignite-coal, better utilized through co-gasification to produce syngas, a clean and environmental friendly fuel, with easier application in engines. Blends of Mui-basin coal (MBC), Prosporis juliflora(PJ), Hyphanae compressa(HC) and rice husk(RH) were cofired with resultant upgraded-syngas operating tricycle engine. Analyzed upgraded-syngas reported improved yields on combustible gases and Hydrogen/Carbon-monoxide ratio (low rank to moderate). Calorific values reported 3.2-11.2% increase. At half-load and relative to neat diesel (ND), peak-pressure improved by 31.6%(MBC-PJ), 24.0%(MBC-HC) and 14.6%(MBC-RH). Additionally, peak-pressure increases as load increases and shifts to the right of top-dead-centre with reported increase of 13.1%MBC-PJ, 15.4%MBC-HC, 18.3 % MBC-RH and 16.5 % for ND. Moreover, Net heat release rate (NHRR) in J/degree increased rapidly at 15-25oafter/TDC for all loads and also increased as the load increased with values of 33.4(HC), 26.8(ND), 28.8(RH) and 37.8(PJ) at no load and 35(HC), 27.8(ND), 30(RH), and 38.9(PJ) at full load condition. The optimal approach for sustainably utilization of MBC is through the novel fuel, in which MBC-PJ ranks the best followed by MBC-HC and lastly MBC-RH.

Keywords: Calorific value, crank angles, syngas, cylinder pressure, net heat release rate, engine load



@ The author(s). Published by CBIORE. This is an open access article under the CC BY-SA license (http://creativecommons.org/licenses/by/4.0/).

Received: 26th March 2024; Revised: 16th April 2024; Accepted: 18th April 2024; Available online: 22th April 2024

1. Introduction

Coal deposits in Mui basin, Kenya are estimated to be 400 million tonnes, which according to Tenge *et al.*, (2013) is a low grade coal. Worldwide, coal accounts for 27% of total energy supplies with 35% of electricity generated through use of coal (Alam *et al.*, 2013; Molino *et al.*, 2018). Coal combustion emits considerable emissions such as carbon dioxide, acidic gases (SOx and NOx) and particulates, leading to pollution (Mutemi Muthangya and David Samoei, 2012). Coal has low hydrogen carbon ratio with high calorific value whereas biomass has high Hydrogen/Carbon ratio with low calorific values. Blending coal and biomass has various advantages as biomass acts as a hydrogen donor to coal and the ash produced can be used as a catalyst (Ozturk & Dincer, 2018). Asaro & Smith, (2013), reported that conventional pulverized combustion plants releases large amounts of emissions such as CO₂, SO_x, NOx and dust where carbon in the fuel is oxidized to CO₂ a greenhouse gas with adverse environmental impacts. According to Barrett, (2011) coal as a solid fuel cannot be applied in internal combustion engines because of difficulties in handling the fuel and disposal of solid residue. Additionally, coal as solid fuel had storage and feeding problems, compared to gaseous and liquid fuels making solid fuels inappropriate as transport fuels. Coal biomass gasification to produce upgraded syngas a clean and environmentally friendly fuel will also have positive impacts to the community (Kamau *et al.*, 2022; Siedlecki & De Jong, 2011).

1.1. Co-gasification of MBC with biomass

Coal biomass gasification referred as co-gasification has several advantages compared to either biomass or coal gasification alone. These advantages includes reduction in CO_2 emission, sulfur and ash which contribute to environmental pollution and corrosion of equipment in coal gasification processes (*Chmielniak and Sciazko, 2003; McLendon et al.,* 2004; Kamble *et al.,* 2018). Blending coal and biomass lowers the cost of feedstock, and tar generated. In addition, biomass has high oxygen content and thus require less external oxygen for gasification when compared to coal. At the same time, biomass sources have comparatively low calorific values than coal, which is not desired in any integrated gasification combined cycles (IGCCs) or power generation plants like ICEs (Ozturk & Dincer, 2018).

To optimize the co-gasification process of coal and biomass, various parameter needs to be considered such as particle sizes and ratio of biomass to coal in the blend. The blending ratio of biomass and coal has an impact on the harmful emission released from gasification process. Additionally, the high volatile in biomass and its high thermochemical reactivity usually facilitate the

_

¹Institute of Energy and Environmental technology, Jomo Kenyatta University of Agriculture & Technology, Nairobi, Kenya

²Department of Physics, Jomo Kenyatta University of Agriculture &Technology P.O. Box 62000-00200, Nairobi, Kenya

³Department of Engineering, Technische Hochschule Brandenburg Magdeburger Str.50, 14770 Brandenburg an der Havel, Germany

⁴Department of Mechanical and Automotive Engineering, Technical University of Mombasa, Kenya

^{*} Corresponding author Email: benswamb@yahoo.com (B. Kariuki)

conversion and the upgrading of the syngas fuel. Therefore, Co-gasification is the optimal and sustainable approach to utilize coal and biomass with minimal environmental pollution.

Syngas composition and its calorific values are important factors in co-gasification. Investigations into the effects of blending ratios and operational conditions has been reported recently; however, the findings are inconclusive, probably due to use of different gasifier designs. Most of the documented research has focused on fluidized-bed gasifiers, primarily because the goal of co-gasification of biomass and coal is to supply a large-scale gasification plant (Hurskainen & Vainikka, 2016). Moreover, depending on syngas application, the oxidizing agents can be varied to produce syngas with desirable composition (Dascomb, 2013). Mixing ratios, selection of gasifier, steam generation, supply of air or oxygen-rich air, optimization of suitable temperature, effective usage of catalyst, and downstream treatment and handling processes require special attention (Kamble *et al.*, 2018). The syngas produced in gasification can be applied in ICEs as well as direct heat applications to replace furnace oil (Reed & Das, 1988).

1.2. Upgraded Syngas as a fuel for internal combustion engines (ICEs)

Various factors affect syngas applications in ICEs, such as; syngas composition, engine load, injection timing and compression ratios (Gatumu, 2021; Stone, 1999). Kamal *et al.*, (2015) reported that syngas contains approximately 40% of carbon monoxide (CO), hydrogen (H₂), and methane (CH₄) which are combustible gases and 60 % non-combustible gases (Nitrogen (N₂), carbon dioxide (CO₂), along with varying proportions of water vapor (H₂O). Hydrogen, a constituent of syngas, possesses clean-burning characteristics, rapid flame propagation, and broader flammability limits. These attributes lead to shorter combustion durations and increased efficiency in Internal Combustion Engines (ICEs). Azimov *et al.*, (2013), reports that there was significant power degrading in the engine and challenges of maintaining and sustaining stable combustion due to variations in syngas composition and low energy density.

Chribik *et al.*, (2012) studied engine load variation and reported that at the low load, the cylinder temperature decreased due to delayed combustion and inefficient oxidation of syngas fuel. They further observed that as engine load increased the cylinder temperature and pressure increased. Hagos *et al.*, (2013), investigated combustion characteristic when injection timing was adjusted in spark ignition engine by varying the crank angle measured BTDC. They reported that optimal combustion occurred at start of injection of 120° BTDC at speed up of 2100 rpm.

There exist various challenges when syngas is to be applied in ICEs such as power de-rating (reduced power output), increased end gas temperature and pressure. Various researchers have addressed these problems. For instance Laurence & Ashenafi, (2012) identified gas cleaning to remove ash, tar and corrosive SOx and NOx gaseous compound as the main requirement for syngas to be applied in ICEs. They noted that tar and ash cause fouling of pipes and heat exchangers, which reduced engine's performance and reliability with higher emissions. They also observed that, the effects of high levels of tar and ash in the syngas lowers engine break thermal efficiency and increases engine emissions particularly the particulate matters. In order to address the problems highlighted while using syngas as a fuel, syngas upgrading through co-gasification, cleaning and cooling as well as engine modification and retrofitting can be applied as solution to the challenges.

1.3. Retrofitting ICEs for syngas fueling

Various researcher reported syngas fuel to be of inferior in quality than that of gasoline and natural gas, necessitating design adjustments such as raising the compression ratio and adjusting the injection timing or ignition timing (Lee & Castaldi, 2010; Pradhan *et al.*, 2015). A study reported that syngas has low flame speed when compared to gasoline and thus to be applied in ICEs there was need to advance ignition timing by about 30-40 degrees (Pradhan *et al.*, 2015). In the experimental setup of direct injection compression ignition (DICI) engines, it may be necessary to incorporate holding device for dual fuel line and install a piezoelectric pressure sensor for pressure data collection (Hagos *et al.*, 2014).

1.4. Syngas combustion characteristics in dual fuel engine

Engines operating on dual fuel have five key stages as shown in Figure 1.

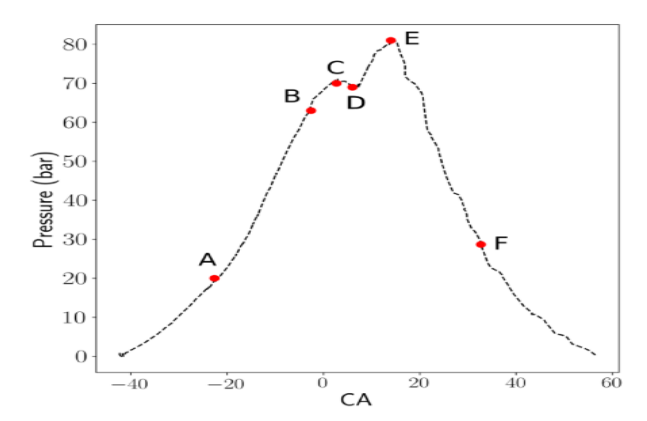


Figure 1 Dual fuel combustion phases Source (Mansor, 2014; Nwafor, 2002)

The initial phase AB occurs after diesel is injected and is characterized by delay in the ignition of the pilot fuel. During this phase, complex chemical reactions occur. For dual-fuel engine, diesel is applied as supplementary fuel (secondary) and syngas as

the main fuel source (primary). There is reported ignition delay time in syngas because the gaseous fuel fraction (which has inert gases) lowers the concentration of oxygen within the spray region thereby slowing the combustion (Fiore *et al.*, 2020; Sombatwong *et al.*, 2013). Typically, the pilot diesel is injected and automatically ignites before top dead center (TDC), creating multiple ignition kernels which occurs prior to combustion. Subsequently, combustion of this premixed fuel occurs leading to a subsequent pressure increase (phase BC) (Azimov *et al.*, 2013; Fiore *et al.*, 2020). The increase in pressure is linked to the combustion of a mixture of air and diesel fuel close to the ignition spot. As the flame disperses from the sprayed region, diesel combustion shifts to a diffusive phase, predominantly governed by fuel mixing rather than chemical kinetics (*Fiore et al.*, 2020). Phase CD is characterized by a pressure drop related to the initial delay period of the primary fuel. Venkatesan & Shangar, (2015) noted a decrease in ignition delay as the load and compression ratio were increased, and also observed minimal delays at full load and at compression ratio of 18.

In phase DE (fourth stage), syngas combustion takes place rapidly which subsequently leads to increase in pressure. Phase EF is characterized by turbulent flame propagation. The combustion in this phase is sustained by contribution of the two fuels. The maximum peak was observed at point E, occurring several degrees after top dead center (TDC) (Azimov *et al.*, 2013).

Hariram & Vagesh Shangar (2015) observed a decrease in ignition delay with increasing load and compression ratio, noting minimal delay at full load and at compression ratio of 18. They also observed that increasing the CR caused the maximum pressure to move slightly closer to top dead center (TDC), with the optimal compression ratio being 18. This phenomenon was attributed to the rise in in-cylinder air temperature and the early onset of combustion, which facilitated a reduction in ignition delay. These findings were supported by research conducted by EL_Kassaby & Nemit_allah (2013), Hariram & Vagesh Shangar (2015), Raj & Kandasamy (2012), and Stone, 1999.

Combustion characteristics are well described using in-cylinder pressure and neat heat release rates. Cylinder pressure is monitored throughout the crankshaft by measuring the angle of rotation on the crankshaft for the power and compression strokes. The cylinder pressure is directly linked to engine efficiency and the power developed during the expansion stroke. The formation of oxides of nitrogen are affected by pressure and temperature in the cylinder (Tesfa *et al.*, 2013). The maximum cylinder pressure increases as the load increases and reduces as compression ratio decreases (Venkatesan & Shangar, 2015). A study by Gatumu *et al.*, (2021), reported a higher in-cylinder pressure for syngas operated CI engine (12.5% higher than standard injection timing of 23 degrees) when the injection timing was advanced with 25.2 degrees crank angle Btdc than retarded to CA 20.8 degrees Btdc (syngas decreased by 26.6% and neat diesel by 29.7%). They attributed this to better fuel combustion in the expansion stroke after TDC. Soni & Gupta, (2015), reported shorter delay period, high in-cylinder pressure and temperature when IT was advanced by a crank angle of 6 to 10 degrees Btdc. Other factors affecting maximum pressure are the engine's compression ratio, combustion duration, net heat release rate (NHRR) and air fuel ratio (AFR) distribution (Kalam & Masjuki, 2011).

The heat release is a measure of the amount of energy released per unit time from the combustion of a fuel which is determined by analyzing the cylinder pressure data relative to the position of the crankshaft (Spaeth, 2012; Vipavanich *et al.*, 2018). Heat release can be used an indicator of completeness of combustion (Heywood, 1988). Equation 1 relates volume change with crank angle (instantaneous volume)(Spaeth, 2012) and when differentiated yields to $\frac{dV}{d\theta}$ a derivative in equation 1. Equation 2 is derived from first law of thermodynamics and can be applied in calculation of net heat release rate (Mulay S.S., 2014).

$$V(\theta) = \frac{v_d}{v_{-1}} + \frac{v_d}{2} \left[(R' + 1 - \cos\theta - (R^2 - \sin^2\theta)^{1/2}) \right]$$
 (1)

Where $v_d = \frac{\pi}{4} (bore)^2 (stroke)$, R is compression ratio and R'= $\frac{2 (length \ of \ connecting \ rod)}{crank \ throw}$

$$\frac{Dq}{d\theta} = \frac{\gamma}{\gamma - 1} p \frac{Dv}{d\theta} + \frac{1}{\gamma - 1} V \frac{dp}{d\theta} \tag{2}$$

Where Q represents the heat released per unit time, θ stands for crankshaft angle, P denotes pressure in the cylinder, V represents volume in cylinder at the instantaneous point, and γ represents the ratio of specific heat. The specific heat ratio is determined by calculating the slope in log P-log V curves for different strokes. $\frac{dp}{d\theta}$ Is obtained as gradient of pressure against crank angle curves, while $\frac{dV}{d\theta}$ is a derivative of equation 1

The values of equation 1 is determined by taking measurement or using the manufacturer manual on engine specifications. The gradient of log P against log V curves at the compression stroke of a 4-stroke engine yields the value of k (ratio of specific heats), which is illustrated in Figure 2.

The NHRR can also be determined by evaluating the fuel chemical energy absorbed into the coolant system. With higher compression ratios (CR), a larger quantity of heat is released (NHRR) during the premixed combustion phase than during the diffusion phase and the higher the CR the better the values of NHRR (Hariram & Vagesh Shangar, 2015). Other studies have shown that increasing compression ratio increases combustion temperatures, which increases cylinder pressures and leads to complete combustion (Mahgoub *et al.*, 2015). Based on the various results by researchers the present study chose 25.2 degree a/TDC to be the optimal injection timing and a compression ratio of 18.

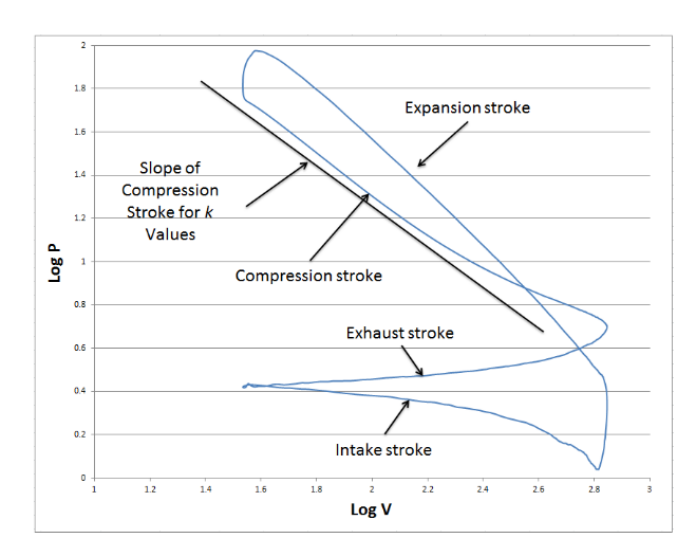


Figure 2. log P against log V showing slope at compression stroke of an otto engine (Spaeth, 2012)

2. Materials and method

2.1. Co-gasification and syngas upgrading for MBC, P. juliflora, H. compressa and rice husk

A fixed bed gasification unit shown in figure 2.1 available at JKUAT was used to gasifier the sample blends. Safety was enhanced by checking for any leaks using ultrasonic leak detector model GS 5800 on all the joints and pipes work on the gasifier and connection to engine. The room ventilation was also checked and all windows opened to avoid carbon monoxide poisoning. Safety boot and other Personal protective equipment were applied on.

Samples of Mui Basin coal were pulverized to small particles and sieved to 3 mm (Dechsiri, 2004). For *Pjuliflora* and *H compressa* the samples were cut into small pieces of 2-3 cm, crushed and sieved to 3 mm and then mixed in a ratio of 1:1 MBC and *P. juliflora*, *H. compressa* and rice husk weight by weight. The samples were then coded as 50% MBC50%, 50% MBC50%HC, and 50%MBC50%RH.

The gasifier unit was fitted with two type K thermocouples located at the port 1 (near ashtray) and port 2 (upper part of combustion chamber) and connected to Advantest multiple digital data recorder model TR2724 for temperature recording. The decker air blower was used which was calibrated using the manometer flow meter where Level 1 was taken as 1.04 m³/min, 2 as 1.48 m³/min, 3 as 2.02 m³/min (which was set and used), 4 as 2.49 m³/min, 5 as 2.98 m³/min and level six (highest) as 3.50 m³/min.

The feedstock was placed at the bottom of the gasifier near the ashtray and ignited. The blower was started slowly from level one, to level two and then set at level 3. The upgraded syngas was passed through quenching water to help solidify the suspended solids (ash, dust and soot) and tar then to fibre clothe and cotton wool filters when still hot to avoid pressure drop and then through cyclone cork filters as shown in Figure 3 (Hagos *et al.*, 2014; Laurence & Ashenafi, 2012). The gas was then cooled using fins with blower to attain room temperature.

2.2. Test Engine modification, retrofitting and adjustment to run on the upgraded syngas

The test engine available at JKUAT and shown in Figure 4 and 5 with specification as 3.5 Kw, multi fuel, Kirloskar-make, 4-stroke, single cylinder, compression ignition, naturally aspirated and water cooled was used in the study. It was modified by retrofitting and adjustment in area such as fuel supply system, injection timing, and compression system. For the fuel system, the design was modified by inclusion of two pipes (T shape); one direction flow valve, pressure regulator, and flow meter to allow syngas and air to the engine. Pilot diesel was injected through fuel injections nozzles. The injection timing was set at 25.2 degrees by manually rotating the flywheel and checking for spill in the high pressure pipe connector of injector pump. The engine compression ratio was set to 18 without changing the geometry of combustion chamber (Mahgoub *et al.*, 2015).

In-cylinder pressure can be determined though measuring the crankshaft angular velocity at a given point (instantaneous angular velocity) or pressure measurement in the firing cylinder using piezo-sensors. The cylinder pressure was monitored using miniature piezo sensors, Models SM111A22 and M108A02 (serving as crank angle sensors), equipped with transducers for dynamic measurement of compression and combustion pressures, as depicted in Figure 6. Additionally, an incremental shaft encoder was employed to determine the engine crankshaft rotation position, providing 360 pulses per revolution. Data from sensors were sent to engine software (ICEngineSoft version.9.0) for decoding, recording and analysis (Mulay *et al.*,2014). The recorded cylinder pressure (p) corresponding to crank angle (θ) positions were used to calculate the engine's heat release rate ($\frac{dQ_n}{d\theta}$) using equations 1 and 2. The test engine was controlled through a control panel which had different sensors like piezo sensor shown in Figure 5. Other engine controls includes speed adjustment, load control and ignition switch for starting the engine. Engine geometrical and operational specification are tabulated in Table 2 and 3.

Table 2. Engine geometrical specifications and features (Mulay., 2014)

Engine parameter	Details		
Make/Model	Kirloskar 4 stroke		
Number of cylinders	Single		
Bore (mm)	87.5		
Rated power (Kw rated at 1500 rpm)	3.5		
Maximum rated power (Kw)	5.8		
Cylinder total volume (cm³)	950		
Connecting rod length (mm)	234		
CR range	12-17.5		
Standard Injection timing (°Btdc)	23		
Loading/Braking	dynamometer Eddy current type		
Load indicator (0-100%)	Digital		
Fuel flow transmitter (mm WC)	Range 0-500		
Temperature sensor	Thermocouple Type K		

Table 3. Engine operational parameter (Mulay, 2014)

Engine operational parameter	Values
Aspiration	natural
Fuel	Diesel/Petrol/Syngas/biodiesel
Stroke length (mm)	110
Torque (Nm)	11.5
Peak pressure (bar)	76
Power output (Kw)	3.5
Swept volume (cm³)	661
Combustion system	Direct injection
Speed (rpm)	1000-1500
Fuel tank capacity (litres)	15



Figure 3. Fixed bed gasifier at JKUAT showing port 1 and 2 (Fernando, 2014; Nduku Nzove, 2021)



Figure 4 Syngas cleaning and cooling unit showing Syngas sampling port



Figure 5. Gasification system and Test engine layout



Figure 6. Detailed test engine and workbench at JKUAT manufactured by Apex pvt. Limited



Figure 7. Piezo sensor to measure in cylinder pressure

2.3. Test running the engine for combustion characteristics

A calibrated flow meter was used to measure and record syngas flow rate then the upgraded syngas was applied to the combustion chamber of the test engine shown in Figure 6 and 7. Upgraded syngas was supplied as main fuel while diesel was supplied as supplementary fuel. The secondary fuel (pilot diesel) was used since the mixture of air and syngas cannot ignite automatically since air syngas auto ignition temperature are high (around 500 degree Celsius) and a small amount of diesel is usually added to assist and boost combustion at the end of compression phase (Mahgoub *et al.*, 2015). This was achieved by choosing an injection timing of 25.2 degrees by suppling accurately measured amount of diesel (determined through crank and piston position). For accurate fuel supply, syngas amount was measured through a flow meter with a control valve and calibrated through a manometer.

The diesel amount was controlled through a flow control valve (fuel cock) and flow governor. The governor increases or decreases the diesel fuel needed in combustion chamber in order to maintain engine output as the variation of energy content in syngas occurs (Bates & Dölle, 2017). The mixing unit was fitted in the system (Gatumu *et al.*, 2021). Prior to starting the engine, water and lubricating oil levels were checked and then the engine was switched on and allowed to run for five minutes at no load condition. Afterwards the engine was test run on different loads (0, 3, 6, 9 and 12 (0, 25%, 50%, 75% and full load) and different samples. (Neat diesel, 50%MBC50%PJ, 50% MBC50%HC and 50%MBC50%RH). The desired engine load was gradually increased and maintained for approximately two minutes to ensure stability. During this time, fuel consumption was measured over one minute, while monitoring

and recording parameters such as torque, speed, various temperatures including exhaust temperatures. This was achieved through use of dynamometer and various sensors, in which data was decoded by inbuilt computer and the output was done through interface software. The software recorded the data and generated some graphs that gave the combustion parameters (NHRR and cylinder pressure). The engine data collection was done in an interval of one minute where data for ten cycles were recorded for the sample and range or average were used for result analysis.

2.4. Combustion characteristic of diesel and upgraded syngas

The piezo-sensor generated combustion parameters which were used to characterize the engine (Hariram & Vagesh Shangar, 2015). These combustion parameters were: in-cylinder pressure, crank angles and net heat release rate obtained using equation 1 and 2. (Vallinayagam *et al.*, 2013; Wekesa, 2013; Zheng *et al.*, 2008).

2.5. Sampling and testing the upgraded syngas

The upgraded syngas was then sampled occasionally at a predetermined time of one-minute (at least three sampling) interval using evacuated gas flask and gas analyser Testo model 350S/-XI with accuracy of $\pm 5\%$. The gas analyser was fitted with sensors for NO, NO₂, SO₂, CO₂, and CO. The probe was inserted in syngas flow valve and readings were recorded in the output screen and in the laptop as percentages or part per million (PPM). For hydrogen, gas chromatograph was used. In this case, a glass flask was evacuated by use of vacuum pump to create a partial vacuum in a prepared solution of 10M Sodium hydroxide. Carbon monoxide and carbon dioxide were absorbed in sodium hydroxide solution and hydrogen, methane, Nitrogen and Oxygen were left for analysis. The GC was first calibrated using pure 99.999% instrument grade hydrogen gas. The samples were then withdrawn by use of 2 ml syringe and injected to input port of Gas chromatograph, Model GC -2014 ATF by Shimadzu Corporation with GC lab solution software interface, available at GDC Menengai, in Nakuru County. The output port of GC was connected to container containing water to discharge excess sample gas. The cooling was done at 11^{th} minute to switch off (bake detector). The carrier gas used was argon. The composition of the upgraded syngas was determined in terms of percentage of carbon monoxide, hydrogen gas, carbon dioxide, water vapour, methane, oxide of Sulphur and Nitrogen as well as Nitrogen gas. Sensors specifications and accuracies for gas analyser testo 350 are presented in Table 4.

Table 4 Gas analyzer Testo 350 model sensors specifications and accuracies

Sensor	Range of composition	Accuracy (%)		
Oxygen sensor	0-21%	±2		
Carbon monoxide	0-5000ppm	±10<400ppm and ±5>400ppm		
Carbon dioxide	0-2000ppm	±0.3		
Hydrocarbon	Upto 21%	±10		
Oxides of nitrogen	0-5000ppm	±5		
Thermocouple type CRAL	0-600°C	±3		

3. Results and result analysis

The derived upgraded syngas and its combustion properties in direct injection compression test engine in terms of cylinder pressure, engine load and net heat release are discussed in details and compared with other researchers' findings.

3.1. Results and results analysis on upgraded syngas

The optimal blends at a ratio of 1:1 (w/w) for *P. juliflora, H. compressa* and rice husk were gasified to yield syngas at a temperature range of 250 to 600 °C. The enhanced syngas was further cooled to ambient temperature. The composition of upgraded syngas is shown in Table 5. Table 5 shows the comparable work done by other researchers.

Table 5. Properties of Syngas as a fuel from 50% Mui Basin Coal -50% biomass

Syngas composition	50%PJ50%MBC	50%HC50%MBC	50%RH50%MBC	P value
CO (%)	24.75±0.56 a	23.8±0.01 b	20.89±0.78°	0.04 ^S
CO ₂ (%)	10.21±0.32 ^d	9.8 ± 0.02^{e}	$15.54 \pm 0.44^{\mathrm{f}}$	0.04^{S}
H ₂ (%)	22.23±0.04 ^g	$18.7 \pm 0.72^{\rm h}$	14.23 ± 0.08^{i}	0.305^{nS}
CH ₄ (%)	2.23 ± 0.07^{j}	2.2 ± 0.86^{k}	5.23 ± 0.06^{1}	0.00 ^s
N ₂ and others*(%)	40.58 ± 0.12^{m}	45.5 ± 0.59^n	44.11±0.18°	0.00^{S}
Calorific values (MJ/m³)	4.97 ± 0.10^{p}	4.78 ± 0.13^{q}	4.61 ± 0.09^{r}	0.02^{S}
Average H ₂ /CO ratio	0.9	0.79	0.68	

smeans significant, non-significant, letters in same row indicate significant differences at the 5% level using Tukey's and Scheffe's test and * is calculated by differences.

Table 6. Comparison between properties of syngas as a fuel from literature and the upgraded syngas

Syngas parameter	Coconut shell ^{1a}	Palm husks ^{2c}	Switch grass downdraft ^{3b}	Indian coal ^{4b}	Prospulis juliflora ^{5a}	Rice husk ^{6a}	Mui basin coal ^{7d}	Prospulis juliflora ^{8b}
CO (%)	17-22	16.6	12-18	41.8	21.15±0.91	16.5- 17.55	18.45	18.4
CO ₂ (%)	10-15	19.2	10-17	0.623	13.15±0.50	14.5-16.1	15.32	13.8
H ₂ (%)	11-14	5.6	7-12	8.8	19.25±0.07	4.1-4.5	6.83	11.1
CH ₄ (%)	1-3	4.3	4.2	17.3	5.45±0.07	6.8-7.2	3.05	2.40
N ₂ and others*(%)	50-60	54	60		40.585±0.19	17.9-54.7	56.35	54.2
Calorific values (MJ/m³)	-	-	-	-	-	-	4.467	4.17-4.85
Average H ₂ /CO ratio	0.64	0.33	0.78	0.21	0.91	0.25	0.37	0.60

1-Bhattacharya & Pham, 2001, 2-Lahijani & Zainal, 2011 3-Kundiyana et al., 2010 4-Raibhole & Sapali, 2012, 5- Gift et al., 2018 6-Njogu et al., 2015, 7-Nduku Nzove, 2021, 8-Nevase et al., 2013, a-Updraft b-downdraft, c-fluidized bed, and d fixed bed *By difference

Statistical analysis from the Table 6, shows that there is statistical difference in mean for the various components of the upgraded syngas for the optimal blend of 1:1 Mui Basin coal to selected biomass. It is also evident that the syngas has been upgraded and has a moderate hydrogen to carbon monoxide ratio at an optimal blending ratio of 1:1. A study by Rath & Longanbach, (1991), classified syngas on the basis of hydrogen to carbon monoxide ratio as low ratio 0.4-0.8, moderate ratio 0.8-1.5 and high ratio as 1.8-2.5. Table 3.2 show comparison of the derived upgraded syngas in reference to other researchers and all had low ratios with *P. juliflora* having a moderate ratio of 0.9. Blending improves the hydrogen carbon monoxide ratio for all Mui basin coal and selected biomass from low ratio to moderate ratio. The low hydrogen to carbon monoxide ratio for rice husk in table 3-2 is due to methanation as the yield of methane is high (Luo, 2017; Rönsch et al., 2016).

The calorific values showed a statistical difference in mean and an improvement of 11.2 % for *P.julifrola*, 7.0 % for *H.compressa*, 3.2 % for Rice husk coal biomass blends when compared with the raw Mui Basin coal. Based on the fluctuations of syngas composition derived from co-gasification the averages shown in Table 6 were considered in analysis of test engine combustion characteristics. Additional the properties presented in Table 7 were considered.

Table 7. Properties of fuel applied in the engine (Mustafa et al., 2017; Nduku Nzove, 2021)

Quantity	Values		
Syngas Temperature at gasifier outlet (°C)	574.8		
Syngas Temperature at cooler outlet (°C)	27		
Atmospheric pressure (bars)	1.013		
Gasifier input temperature (°C)	800		
Syngas pressure at gasifier outlet (bar)	8.5		
Diesel density at 25 °C (kg/m³)	845		
Diesel flow rate (m³/s)	4.56×10^{-7}		
Diesel calorific values (MJ/kg)	42		
Syngas and air flow rate to the engine (m ³ /s)	$4.43X10^{-3}$		
Syngas and Air temperature at inlet (°C)	29.0		
Syngas and Air velocity to engine inlet (mixer) (m/s)	15.5		
Syngas and air density (kg/m³)	0.95		

3.2. Results on in-cylinder pressure

Figure 8 present the variation of pressure in the combustion cylinder at different crank angle before and after top dead centre while the engine was operated at 50 % engine load. High In-cylinder pressure measured in degrees per crank angle produces audible sound referred to as diesel knock in engines and it is represented in figure 3.1, where the peak values are noted with falls before and after TDC. The start of combustion (SOC) for upgraded syngas is recognized by a kink in the curve and end of combustion (EOC) by a plateau. The ignition delay time was high since the upgraded syngas reduced the oxygen concentrations within the spray region and thus slows the burning properties (Fiore *et al.*, 2020; Sombatwong *et al.*, 2013). The higher peaks recorded for 50 % engine load were 56.9 bars at crank angle 15 degrees, 53.6 bars at crank angle 15 degrees and 43.2 bars at crank angle of 4 degrees for *P. juliflora*, *H. compressa*, Rice husk and neat diesel respectively. The values of peak cylinder pressure when compared to neat diesel improved by 31.6% for *P. juliflora*, 24.0% for *H. compressa*, and 14.6% for rice husks and the peak shifted to the right of top dead centre due to the exhibited delay in combustion of upgraded-syngas. The study shows that upgraded syngas has a higher peak than standard neat diesel with injection timing of 23 degrees. This means that upgraded syngas has better combustion characteristic due to presence of dual fuel in the engine. Cylinder pressure is influenced by the rate of fuel combustion during the premixed burning phase. Moreover, as the quantity of fuel blends increases, more fuel contributes to the uncontrolled combustion stage of the mixture, leading to a higher increase in pressure (Kale, 2017; Velmurugan *et al.*, 2014).

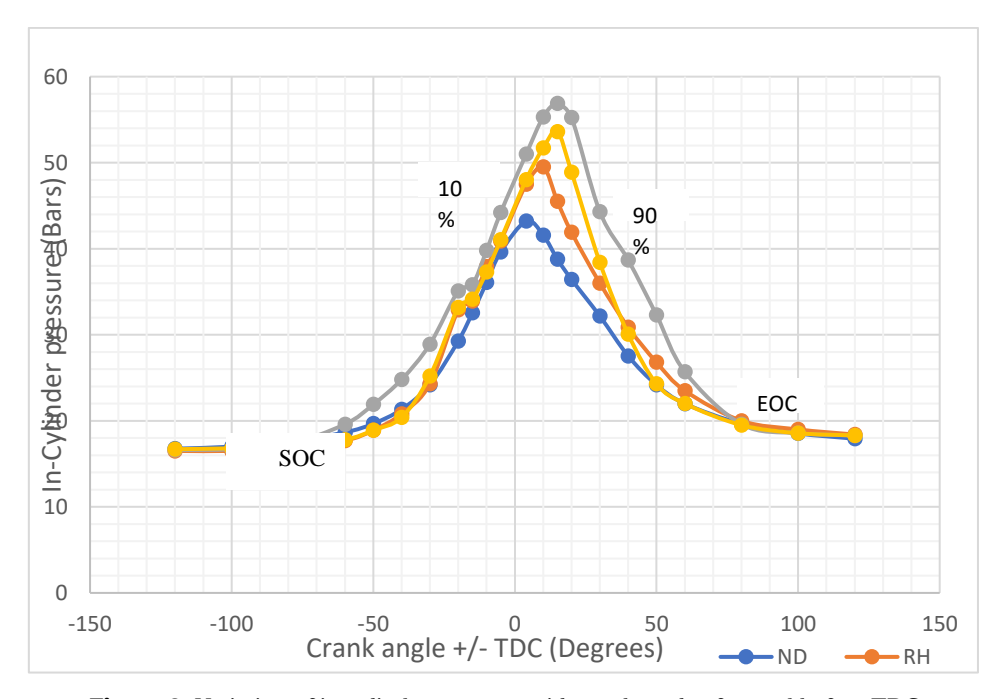


Figure 8. Variation of in-cylinder pressure with crank angle after and before TDC

The maximum peak (cylinder pressure) for diesel was at 4 degrees at TDC with the dual fuel shifting with more than 10 degrees to the right after TDC. The peak for syngas shifted toward expansion stroke due to late combustion of syngas. A study by Lal & Mohapatra, (2017), reported maximum cylinder pressure of 46.53 bar and 55.29 bar at crank angles of 12 and 14 degrees for diesel and syngas respectively, after top dead center (ATDC) with CR of 18. A research by Sombatwong *et al.*, (2013) reported a peak pressure of 56.5 bar when the engine was operated on dual fuel and 55.0 bar when operated on diesel at a CR of 18. Similarly, Sahoo *et al.*, (2012), reported maximum cylinder pressure of 51.7 bar for a 50 % hydrogen syngas, when the engine was operated at maximum efficiency. They further noted that at low loads of 20-40%, there were low cylinder pressure due to reduced quantity of pilot fuel that resulted to slower combustion rates. Other studies has also shown the maximum in-cylinder pressure peaks moves to after the TDC when syngas and diesel are used as fuel (Brusca *et al.*, 2014; Dhavale *et al.*, 2015). The higher gaseous fuel content in syngas that burns at higher rates resulted to high pressure rise in the engine than when compared to conventional diesel (Ashok & Nanthagopal, 2019).

3.3. Variation of net heat release with the crank angle

Net heat release rate curves are important as combustion parameter like combustion duration (time taken to combust from 10% to 90% of mixture) and intensity can be calculated and analyzed. Figure 9 shows the variation of net heat release (J/degree) with the crank angle a/bTDC (degrees) for 50 % engine load condition.

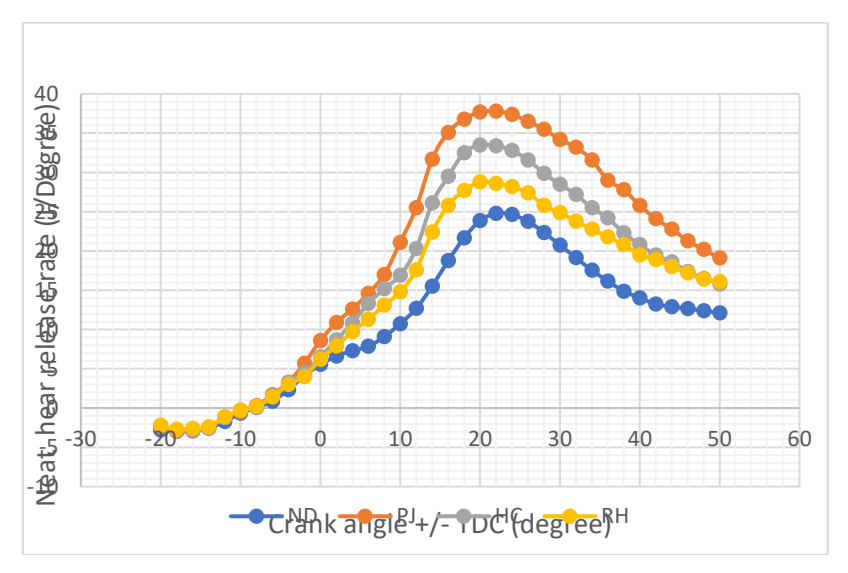


Figure 9. Variation of net heat release with crank angle a/b TDC at 50 % engine load

From Figure 9, the data shows a rapid increase of heat release curve at an angle of 15-25 degrees a/TDC during the period when turbulent flame propagation occurs (spontaneous flame propagation). The start of combustion can be noted by the change from negative NHRR to zero. The low heat release values seen in the graph between -10 to 10 degrees crank angle are attributed to the cooling on the mixtures caused by their interaction with the engine surfaces, as well as the expansion they undergoes (Dhavale *et al.*, 2015). For *P. juliflora* the values for NHRR at 50 % engine load, increased rapidly from start of combustion at 0.3 to maximum of 37.8 J/degree, *H. compressa* increased from 0.2 to a maximum of 33.5 J/degree, Rice husk increased from 0.2 to 28.8 J/degree and for neat diesel it increased from 0.1 to 24.8 J/degree. Table 8 present the peaks for NHRR curves for the various engine loads.

Table 8. Net heat release rate (J/degree) at various engine load in percentage

Sample name	0 % engine load	25 % engine load	50 % engine load	75 % engine load	100% engine load
НС	33.4	34.6	34	35.2	35
ND	26.8	27.4	27	27.6	27.8
RH	28.8	29.3	29.12	29.8	30
PJ	37.8	38.8	38.82	38.84	38.9

From the Table 8, there is a slight increase in NHRR as the engine load increase. A study by Hariram & Vagesh Shangar, (2015) reported similar findings with maximum heat release of 23.1 J/CA under no load condition and 39.4 J/CA at 50% engine load at CR of 18. Syngas had higher values of NHRR due to the extended crank interval for the combustion of the upgraded syngas fuel and thus better combustion duration. The diesel fuel auto ignites the syngas but has minimal contribution to net heat release (Spaeth, 2012). From the graphs, it can also be noted that there is a slow flame propagation followed by a rapid flame propagation, which is caused by delayed combustion in syngas. This implies that heat release is a spontaneous and short duration occurrence with uncontrolled flame propagation. A study by Mahgoub *et al.*, (2015) on DICI engine, running on dual fuel and simulated using hydrogen derived syngas, reported similar patterns. They attributed this to better flame propagation in hydrogen at leaner modes of fuel mixtures. The syngas seems to have better heat release than diesel because of the presences of more fuel in combustion chamber. At compression ratio of 18, Lal & Mohapatra, (2017), reported NHRR of 32.76 J/deg CA for engine operated on diesel and 46.93 J/deg CA for dual fuel (Syngas and diesel). Sombatwong *et al.*, (2013), also at compression ratio of 18, observed NHRR to be a maximum of 35.0 J/deg crank angle when operated on diesel and 40.0 J/degree crank angle for dual fuel.

3.4. Variation of peak In-cylinder pressure (Bars) with Engine load

Figure 10 present variation of in-cylinder pressure with the engine load. It is evident that the peak cylinder pressure increases from no load condition to a peak cylinder pressure at full load condition.

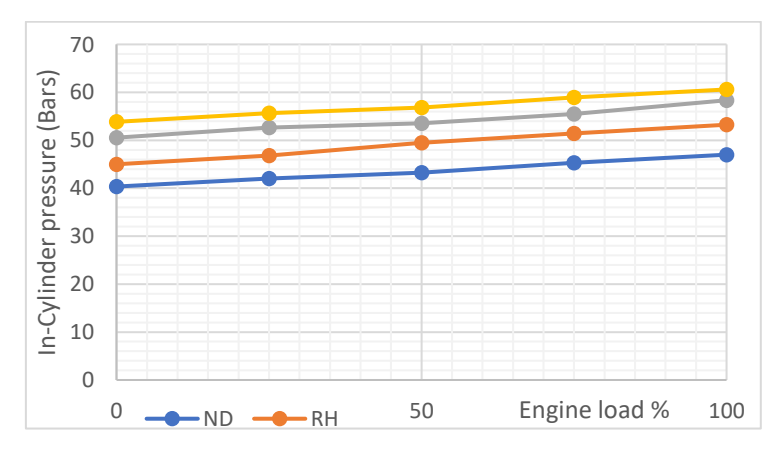


Figure 10 Variation of peak in cylinder pressure in bars with engine load

Neat diesel had the lowest peak cylinder pressure while *P. juliflora* had the highest. The in-cylinder pressure increased from 40.35 bar at no load to 47 bar at full load for neat diesel (16.5 % increase). For *P. juliflora* it increased from 53.85 bar at no load to 60.6 bars at full load (13.1 % increase); 50.55 bar at no load to 58.35 bar at full load for *H. compressa* (15.4% increase), and 45 bar at no load to 53.25 bar at full load for rice husks (18.3 % increase). A study investigating the impact of the hydrogen to carbon monoxide ratio in syngas fuel operated on dual fuel mode observed similar results. They noted as the engine load increased from 20% to full load, there was an increase in peak cylinder pressure (Sahoo *et al.*, 2012). Similarly, Hariram & Vagesh Shangar, (2015) reported peak cylinder pressure of 54.9 bar at no load condition, 64.7 bars at 50% engine load, and 70 bar at full load conditions with a compression ratio of 18.

4. Conclusions

Co-gasification improved combustible gases yields, hydrogen/carbon-monoxide ratio and reduced pollutants. The upgraded-syngas in the research ranked as a moderate ratio fuel. Calorific values reported 3.2-11.2% increase with improved peak-cylinder pressure, NHRR at no load and at full load conditions. Unique combustion characteristics noted for NHRR at 15-25°a/TDC are due to the spontaneous and uncontrolled flame propagation occurrence. Additionally, peak-pressure shifted to the right of top-dead-centre due to delayed combustion of the upgraded-syngas. Mui-Basin-coal-*P.juliflora* ranks the best followed by Mui-Basin-coal –*H.compressa* and lastly Mui-Basin-coal-Rice-husk. Co-gasification is the optimal approach to utilize Mui-Basin-coal and biomass in tricycles with minimal environmental pollution.

Conflict of Interest

The authors declare that they have no conflicts of interest.

Data Availability

The data used to in this research study are included within the article and can be provided upon request to the corresponding author.

Acknowledgements

The study was supported by the Technical University of Mombasa through postgraduate scholarship. The authors also acknowledge the Ministry of Energy, Kenya, for the assistance offered in the acquisition of the samples.

References

- Alam, M. S., Wijayanta, A. T., Nakaso, K., & Fukai, J. (2013). Syngas Production from Coal Gasification with CO2 Rich Gas Mixtures BT Cleaner Combustion and Sustainable World (H. Qi & B. Zhao (eds.); pp. 1103–1108). Springer Berlin Heidelberg.
- Asaro, M., & Smith, R. M. (2013). Coal to Liquids Technologies. In Fossil Energy. https://doi.org/10.1007/978-1-4614-5722-0_11
- Ashok, B., & Nanthagopal, K. (2019). 15 Eco friendly biofuels for CI engine applications. In K. B. T.-A. in E.-F. for a S. E. Azad (Ed.), Woodhead Publishing Series in Energy (pp. 407–440). Woodhead Publishing. https://doi.org/https://doi.org/10.1016/B978-0-08-102728-8.00015-2
- Azimov, U., Tomita, E., & Kawahar, N. (2013). Combustion and Exhaust Emission Characteristics of Diesel Micro-Pilot Ignited Dual-Fuel Engine. In Diesel Engine Combustion, Emissions and Condition Monitoring. https://doi.org/10.5772/54613
- Barrett, S. (2011). European Expert Group reports on Future Transport Fuels. Fuel Cells Bulletin, 2011, 12–16. https://doi.org/10.1016/S1464-2859(11)70096-7
- Bates, R., & Dölle, K. (2017). Syngas use in internal combustion engines-A review. Advances in Research, 10(1), 1-8.
- Bhattacharya, S. C., & Pham, H.-L. (2001). A study on a multi-stage hybrid gasifier-engine system. Biomass and Bioenergy, 21(6), 445-460.
- Brusca, S., Chiodo, V., Galvagno, A., Lanzafame, R., & Garrano, A. M. C. (2014). Analysis of reforming gas combustion in Internal Combustion Engine. Energy Procedia, 45, 899–908.
- Chmielniak, T., & Sciazko, M. (2003). Co-gasification of biomass and coal for methanol synthesis. Applied Energy, 74(3–4). https://doi.org/10.1016/S0306-2619(02)00184-8
- Chmielniak, T., Sciazko, M., McLendon, T. R., Lui, A. P., Pineault, R. L., Beer, S. K., Richardson, S. W., Roberts.E, Kulkarni, M., Bhatwadekar, S., Thakur, H., Heragu, S. S., Kusiak, A., Braglia, M., Kusiak, A., Heragu, S. S., Ernawati, D., Rahmawati, N., Pudji, E., ... Farahani, R. Z. (1996). Facilities Planning. INTERNATIONAL JOURNAL OF ENGINEERING SCIENCES & RESEARCH TECHNOLOGY, 1, 62.
- Chribik, A., Polóni, M., & Lach, J. (2012). Effect of gas mixture composition on the parameters of an internal combustion engine. Acta Polytechnica, 52(3). https://doi.org/10.14311/1540
- Dascomb, J. (2013). Thermal Conversion Eciency of Producing Hydrogen Enriched Synthesis Gas from Steam Biomass Gasification. Florida State University.
- $Dechsiri,\,C.\,\,(2004).\,\,Particle\,\,transport\,\,in\,\,fluidized\,\,beds:\,\,experiments\,\,and\,\,stochastic\,\,models.$
- Dhavale, A. A., Kolekar, A. H., & Jadhav, K. M. (2015). An Experimental Investigation and Analysis for Engine Performance, Combustion and Emissions of Dual Fuel CI Engine. International Engineering Research Journal (IERJ), 2, 1215–1224.
- EL_Kassaby, M., & Nemit_allah, M. A. (2013). Studying the effect of compression ratio on an engine fueled with waste oil produced biodiesel/diesel fuel. Alexandria Engineering Journal, 52(1), 1–11.
- Fernando, R. (2014). Developments in modelling and simulation of coal gasifi cation. A Clean Coal Cent., IE no. CCC/232, 1-77.
- Fiore, M., Magi, V., & Viggiano, A. (2020). Internal combustion engines powered by syngas: A review. Applied Energy, 276, 115415.
- Gatumu, J. N. (2021). Evaluation of Combustion, Performance and Emission of a Direct Injection Compression Ignition (DICI) Engine Running on a Diesel-Syngas blend. JKUAT-COETEC.
- Gift, G. K., Njogu, P., & Kinyua, R. (2017). Comparative Studies of the Energy Properties for Prosopis juliflora and Rice Husks (Oryza sp.) as Feedstock for Renewable Energy Generation. International Journal of Science and Research (IJSR), 6(4), 1569–1572.
- Gift, G. K., Njogu, P., & Kinyua, R. (2017). Comparative Studies of the Energy Properties for Prosopis juliflora and Rice Husks (Oryza sp.) as Feedstock for Renewable Energy
- Hagos, F. Y., A., R. S., & A., A. and S. (2013). Study of Syngas Combustion Parameters Effect on Internal Combustion Engine. Asian Journal of Scientific Research, 6, 187-196.
- Hagos, F. Y., Aziz, A. R. A., & Sulaiman, S. A. (2014). Trends of syngas as a fuel in internal combustion engines. In Advances in Mechanical Engineering (Vol. 2014). https://doi.org/10.1155/2014/401587
- Hariram, V., & Vagesh Shangar, R. (2015). Influence of compression ratio on combustion and performance characteristics of direct injection compression ignition engine. Alexandria Engineering Journal, 54(4), 807–814. https://doi.org/https://doi.org/10.1016/j.aej.2015.06.007
- Heywood, J. B. (2018). Internal combustion engine fundamentals. McGraw-Hill Education.
- Hurskainen, M., & Vainikka, P. (2016). 7 Technology options for large-scale solid-fuel combustion (J. B. T.-F. F. E. G. Oakey (Ed.); pp. 177–199). Woodhead Publishing. https://doi.org/https://doi.org/10.1016/B978-1-78242-378-2.00007-9
- Kalam, M. A., & Masjuki, H. H. (2011). An experimental investigation of high performance natural gas engine with direct injection. Energy, 36(5), 3563–3571.

- Kale, P. (2017). Combustion of biodiesel in CI engine. International Journal of Applied Research, 3, 145-149.
- Kamal, B., Mahgoub, M., Hassan, S., & Sulaiman, S. A. (2015). Effect of varying engine parameters and syngas composition on the combustion characteristics, performance and emission of syngas diesel dual fuel engine A review. ARPN J. Eng. Appl., 10(17), 7712–7718.
- Kamau, Antony N., Paul Njogu, Robert Kinyua, and Mohamed Sessay. "Sustainability challenges and opportunities of generating biogas from water hyacinth in Ndunga Village, Kenya." In Proceedings of the Sustainable Research and Innovation Conference, pp. 14-22. 2022.
- Kamble, A. D., Saxena, V. K., Chavan, P. D., & Mendhe, V. A. (2018). Co-gasification of coal and biomass an emerging clean energy technology: Status and prospects of development in Indian context. International Journal of Mining Science and Technology, 1–16. https://doi.org/https://doi.org/10.1016/j.ijmst.2018.03.011
- Kundiyana, D. K., Huhnke, R. L., & Wilkins, M. R. (2010). Syngas fermentation in a 100-L pilot scale fermentor: Design and process considerations. Journal of Bioscience and Bioengineering, 109(5), 492–498.
- Lahijani, P., & Zainal, Z. A. (2011). Gasification of palm empty fruit bunch in a bubbling fluidized bed: a performance and agglomeration study. Bioresource Technology, 102(2), 2068–2076.
- Lal, S., & Mohapatra, S. K. (2017). The effect of compression ratio on the performance and emission characteristics of a dual fuel diesel engine using biomass derived producer gas. Applied Thermal Engineering, 119, 63–72. https://doi.org/https://doi.org/10.1016/j.applthermaleng.2017.03.038
- Laurence, L. C., & Ashenafi, D. (2012). Syngas treatment unit for small scale gasification Application to IC engine gas quality requirement. Journal of Applied Fluid Mechanics, 5(1). https://doi.org/10.36884/jafm.5.01.11963
- Lee, J., & Castaldi, M. (2010). A Study on Performance and Emissions of a 4-Stroke IC Engine Operated on Landfill Gas With Syngas Addition. https://doi.org/10.1115/NAWTEC18-3565
- Luo, Z. (2017). Coal-to-liquids and polygeneration using low rank coals. In Low-Rank Coals for Power Generation, Fuel and Chemical Production (pp. 241-268). Woodhead Publishing.
- Mahgoub, B. K. M., Sulaiman, S. A., Karim, Z. A. A., & Hagos, F. Y. (2015). Experimental study on the effect of varying syngas composition on the emissions of dual fuel CI engine operating at various engine speeds. IOP Conference Series: Materials Science and Engineering, 100(1), 12006.
- Mahgoub, B. K. M., Sulaiman, S. A., & Karim, Z. A. A. (2015). Performance study of imitated syngas in a dual-fuel compression ignition diesel engine. International Journal of Automotive and Mechanical Engineering, 11, 2282.
- Mansor, W. N. W. (2014). Dual fuel engine combustion and emissions-an experimental investigation coupled with computer simulation. Colorado State University.
- McLendon, T. R., Lui, A. P., Pineault, R. L., Beer, S. K., & Richardson, S. W. (2004). High-pressure co-gasification of coal and biomass in a fluidized bed. Biomass and Bioenergy, 26(4). https://doi.org/10.1016/j.biombioe.2003.08.003
- Molino, A., Larocca, V., Chianese, S., & Musmarra, D. (2018). Biofuels Production by Biomass Gasification: A Review. Energies, 11(4). https://doi.org/10.3390/en11040811
- Monteiro, E., Bellenoue, M., Sottton, J., & Rouboa, A. (2012). Syngas Application to Spark Ignition Engine Working Simulations by Use of Rapid Compression Machine.
- Monteiro, E., Sotton, J., Bellenoue, M., Moreira, N. A., & Malheiro, S. (2011). Experimental study of syngas combustion at engine-like conditions in a rapid compression machine. Experimental Thermal and Fluid Science, 35(7). https://doi.org/10.1016/j.expthermflusci.2011.06.006 Mulay S.S. (2014). User Manual for ICEngineSoft.
- Ozturk Muthui, K, R., Kabugu, M., Akisa, D. M., & Rop, B. K. (2014). Coal handling and equipment selection in mui basin, kitui county, kenya. Proceedings of International Conference on Sustainable Research and Innovation, 5, 87–90.
- Mustafa, A., Calay, R. K., & Mustafa, M. Y. (2017). A techno-economic study of a biomass gasification plant for the production of transport biofuel for small communities. Energy Procedia, 112, 529–536.
- Nduku Nzove, S. (2021). Development and Evaluation of Performance of a Bench Scale Gasi er for Sub-Bituminous Coal. JKUAT-COETEC.
- Nevase, S. S., Gangde, C., Gangil, S., & Dubey, A. K. (2013). Assessment of down draft gasifier on Prosopis juliflora. International Agricultural Engineering Journal, 22, 1–7.
- Njogu, P., Kinyua, R., Muthoni, P., & Nemoto, Y. (2015). Thermal gasification of rice husks from rice growing areas in Mwea, Embu County, Kenya. Smart Grid and Renewable Energy, 6(5), 113-119.
- Nwafor, O. M. I. (2002). Knock characteristics of dual-fuel combustion in diesel engines using natural gas as primary fuel. Sadhana, 27, 375-382.
- Nwafor, O. M. I. (2000). Effect of choice of pilot fuel on the performance of natural gas in diesel engines. Renewable Energy, 21(3), 495–504. https://doi.org/https://doi.org/10.1016/S0960-1481(99)00132-9
- Pradhan, A., Baredar, P., Kumar, & Anil. (2015). Syngas as An Alternative Fuel Used in Internal Combustion Engines: A Review. Journal of Pure and Applied Science & Technology, 5(2).
- Raibhole, V., & Sapali, S. (2012). Simulation and Parametric Analysis of Cryogenic Oxygen Plant for Biomass Gasification. Mechanical Engineering Research, 2. https://doi.org/10.5539/mer.v2n2p97
- Raj, M. T., & Kandasamy, M. K. K. (2012). Tamanu oil-an alternative fuel for variable compression ratio engine. International Journal of Energy and Environmental Engineering, 3, 1–8.
- RATH, L. K., & LONGANBACH, J. R. (1991). A Perspective on Syngas from Coal. Energy Sources, 13(4), 443–459. https://doi.org/10.1080/00908319108909001
- Reed, T. B., & Das, A. (1988). Handbook of biomass downdraft gasifier engine systems. Biomass Energy Foundation.
- Rönsch, S., Schneider, J., Matthischke, S., Schlüter, M., Götz, M., Lefebvre, J., Prabhakaran, P., & Bajohr, S. (2016). Review on methanation–From fundamentals to current projects. Fuel, 166, 276–296.
- Sahoo, B. B., Sahoo, N., & Saha, U. K. (2012). Effect of H2: CO ratio in syngas on the performance of a dual fuel diesel engine operation. Applied Thermal Engineering, 49, 139–
- Siedlecki, M., & De Jong, W. (2011). Biomass gasification as the first hot step in clean syngas production process—gas quality optimization and primary tar reduction measures in a 100 kW thermal input steam—oxygen blown CFB gasifier. Biomass and Bioenergy, 35, S40-S62.
- Sombatwong, P., Thaiyasuit, P., & Pianthong, K. (2013). Effect of Pilot Fuel Quantity on the Performance and Emission of a Dual Producer Gas–Diesel Engine. Energy Procedia, 34, 218–227. https://doi.org/https://doi.org/10.1016/j.egypro.2013.06.750
- Spaeth, C. T. (2012). Performance characteristics of a diesel fuel piloted syngas compression ignition engine. Queen's University (Canada).
- Stone, R. (1999). Introduction to internal combustion engines (Vol. 3). Springer.
- Tesfa, B., Mishra, R., Zhang, C., Gu, F., & Ball, A. D. (2013). Combustion and performance characteristics of CI (compression ignition) engine running with biodiesel. Energy, 51, 101–115.
- Testo 350. (2022). https://www.testo.com/en-VN/testo-350/p/0632-3510
- Vallinayagam, R., Vedharaj, S., Yang, W. M., Lee, P. S., Chua, K. J. E., & Chou, S. K. (2013). Combustion performance and emission characteristics study of pine oil in a diesel engine. Energy, 57, 344–351.

- Velmurugan, A., Loganathan, M., & Gunasekaran, E. J. (2014). Experimental investigations on combustion, performance and emission characteristics of thermal cracked cashew nut shell liquid (TC-CNSL)—diesel blends in a diesel engine. Fuel, 132, 236–245.
- Venkatesan, H., & Shangar, R. (2015). Influence of compression ratio on combustion and performance characteristics of direct injection compression ignition engine. Alexandria Engineering Journal, 46. https://doi.org/10.1016/j.aej.2015.06.007
- Vipavanich, C., Chuepeng, S., & Skullong, S. (2018). Heat release analysis and thermal efficiency of a single cylinder diesel dual fuel engine with gasoline port injection. Case Studies in Thermal Engineering, 12, 143–148.
- Wekesa, A. N. (2013). Using GIS to assess the potential of crop residues for energy generation in Kenya [University of canterbury]. https://ir.canterbury.ac.nz/bitstream/handle/10092/7838/Wekesa_Use_of_thesis_form.pdf?sequence=2&isAllowed=y
- Zheng, M., Mulenga, M. C., Reader, G. T., Wang, M., Ting, D. S. K., & Tjong, J. (2008). Biodiesel engine performance and emissions in low temperature combustion. Fuel, 87(6), 714–722.



© 2024. The Author(s). This article is an open access article distributed under the terms and conditions of the Creative Commons Attribution 4.0 (CC BY) International License (http://creativecommons.org/licenses/by/4.0/)